Size and Shape Control of $SrTiO_3$ Particles Grown by Epitaxial Self-Assembly

Vincenzo R. Calderone,[†] Andrea Testino,[†] Maria Teresa Buscaglia,[‡] Marta Bassoli,[‡] Carlo Bottino,[‡] Massimo Viviani,[‡] Vincenzo Buscaglia,*[,‡] and Paolo Nanni[†]

Department of Process and Chemical Engineering, University of Genoa, I-16129 Genoa, Italy, and Institute for Energetics and Interphases, Department of Genoa, National Research Council, I-16149 Genoa, Italy

Received November 24, 2005. Revised Manuscript Received January 23, 2006

Cubic $SrTiO_3$ particles are obtained by precipitation from an aqueous gel suspension. The gel suspension is prepared by hydrolyzing a $TiOCl_2$ solution with NaOH and adding $SrCl_2$. The addition of citric acid leads to spherical particles. The particle size can be tailored in the range 80−1400 nm by varying the temperature and the concentration. A careful control of the synthesis conditions is essential for producing particles with a narrow size distribution. The results of HRTEM and ED investigations provide strong evidence that the oriented aggregation of small (4−5 nm) nanocrystals is the dominant growth mechanism for the formation of the observed $SrTiO_3$ particles. The primary nanocrystals self-assemble in a highly oriented fashion, producing defective single-crystal particles. The above results show that the directional aggregation process can be controlled by changing the temperature and concentration of the suspension as well as by adding organic molecules, obtaining $SrTiO_3$ particles with a controlled size and shape.

1. Introduction

Strontium titanate, $SrTiO_3$, is considered to be a promising material for tunable microwave applications because of its high dielectric constant (ϵ_r), high dependence of ϵ_r on the applied field, and low losses.[1] $SrTiO_3$ is an incipient ferroelectric (or quantum paraelectric)[2] in which a ferroelectric phase can be induced at low temperature by isotopic substitution or substitutional impurities as well as by an external stress.[3−5] Recently, $SrTiO_3$ has been the object of widespread interest for the fabrication of solid oxide electronic devices.[6] Strontium titanate has been also investigated as a photocatalyst[7] and as material for dye-sensitized solar cells.[8]

The dielectric properties and the polarization of ferroelectric and related materials are very sensitive to the morphology and size of the system.[9] Therefore, the ability to tune in a reproducible way the size and shape of $SrTiO_3$ particles is critical for fundamental studies as well as for the preparation of ceramics and composite materials with tailored properties. In addition to the standard solid-state route, several chemical methods have been reported for the synthesis of submicrometer and nanosized $SrTiO_3$ particles: molten salt synthesis,[10] microemulsion-mediated synthesis,[11] Pechini and related methods,[12] thermal decomposition of suitable precursors,[13] decomposition of bimetallic alkoxide precursors in organic solvents,[14] dissolution of metallic strontium in benzyl alcohol and reaction with titanium isopropoxide,[15] hydro-

* To whom correspondence should be addressed. E-mail: v.buscaglia@ge.ieni.cnr.it.

[†] Department of Process and Chemical Engineering.

[‡] Institute for Energetics and Interphases.

(1) Tagantsev, A. K.; Sherman, V. O.; Astafiev, K. F.; Venkatesh, J.; Setter, N. *J. Electroceram.* **2003**, *11*, 5.

(2) Müller, K. A.; Burkard, H. *Phys. Rev. B* **1979**, *19*, 3593.

(3) Itoh, M.; Wang, R.; Inaguma, Y.; Yamaguchi, T.; Shan, Y. J.; Nakamura, T. *Phys. Rev. Lett.* **1999**, *82*, 3540.

(4) Bednorz, J. G.; Müller, K. A. *Phys. Rev. Lett.* **1984**, *52*, 2289.

(5) Haeni, J. H.; Irvin, P.; Chang, W.; Uecker, R.; Reiche, P.; Li, Y. L.; Choudhury, S.; Tian, W.; Hawley, M. E.; Craigo, B.; Tagantsev, A. K.; Pan, X. Q.; Streiffer, S. K.; Chen, L. Q.; Kirchoefer, S. W.; Levy, J.; Schlom, D. G. *Nature* **2004**, *430*, 758.

(6) Pellegrino, L.; Pallecchi, I.; Marrè, D.; Bellingeri, E.; Siri, S. *Appl. Phys. Lett.* **2002**, *81*, 3849.

(7) (a) Domen, K.; Naito, S.; Onishi, T.; Tamaru, K.; Soma, M. *J. Phys. Chem.* **1982**, *86*, 3657. (b) Miyauchi, M.; Nakajima, A.; Fujishima, A.; Hashimoto, K.; Watanabe, T. *Chem. Mater.* **2000**, *12*, 3. (c) Kato, H.; Kudo, A. *J. Phys. Chem. B* **2002**, *106*, 5029. (d) Konta, R.; Ishii, T.; Kato, H.; Kudo, A. *J. Phys. Chem. B* **2004**, *108*, 8992. (e) Miyauchi, M.; Takashio, M.; Tobimatsu, H. *Langmuir* **2004**, *20*, 232.

(8) (a) Burnside, S.; Moser, J.-E.; Brooks, K.; Grätzel, M.; Cahen, D. *J. Phys. Chem. B* **1999**, *103*, 9328. (b) Lenzmann, F.; Krueger, J.; Burnside, S.; Brooks, K.; Grätzel, M.; Gal, D.; Rühle, S.; Cahen, D. *J. Phys. Chem. B* **2001**, *105*, 6347.

(9) (a) Shaw, T. M.; Trolier-McKinstry, S.; McIntyre, P. C. *Annu. Rev. Mater. Sci.* **2000**, *30*, 263. (b) Scott, J. F.; Morrison, F. D.; Miyake, M.; Zubko, P.; Lou, X.; Kugler, V. M.; Rios, S.; Zhang, M.; Tatsuta, T.; Tsuji, O.; Leedham, T. J. *J. Am. Ceram. Soc.* **2005**, *88*, 1691. (c) Rüdiger, A.; Schneller, T.; Roelofs, A.; Tiedke, S.; Schmitz, T.; Waser, R. *Appl. Phys. A* **2005**, *80*, 1247. (d) Naumov, I. I.; Bellaiche, L.; Fu, H. X. *Nature* **2004**, *432*, 737. (e) Zhao, Z.; Buscaglia, V.; Viviani, M.; Buscaglia, M. T.; Mitoseriu, L.; Testino, A.; Nygren, M.; Johnsson, M.; Nanni, P. *Phys. Rev. B* **2004**, *70*, 024107.

(10) (a) Battisha, I. K.; Speghini, A.; Polizzi, S.; Agnoli, F.; Bettinelli, M. *Mater. Lett.* **2002**, *57*, 183. (b) Mao, Y.; Banerjee, S.; Wong, S. S. *J. Am. Chem. Soc.* **2003**, *125*, 15718. (c) Liu, H.; Sun, X.; Zhao, Q.; Xiao, J.; Ouyang, S. *Solid-State Electron.* **2003**, *47*, 2295. (d) Mao, Y.; Wong, S. S. *Adv. Mater.* **2005**, *17*, 2194. (e) Ebrahimi, M. E.; Allahverdi, M.; Safari, A. *J. Am. Ceram. Soc.* **2005**, *88*, 2129.

(11) (a) Perrot-Sipple, F.; Aymes, D.; Niepce, J.-C.; Perriat, P. *C. R. Acad. Sci., Ser. IIc: Chim.* **1999**, *2* (7−8), 379. (b) Li, Y. F.; Lai, Q. Y. *Chin. J. Inorg. Chem.* **2005**, *21*, 915.

(12) (a) Leite, E. R.; Varela, J. A.; Longo, E.; Paskocimas, C. A. *Ceram. Int.* **1995**, *2*, 153. (b) Kakihana, M.; Okubo, T.; Arima, M.; Nakamura, Y.; Yashima, M.; Yoshimura, M. *J. Sol-Gel Sci. Technol.* **1998**, *12*, 95. (c) Arya, P. R.; Jha, P.; Ganguli, A. K. *J. Mater. Chem.* **2003**, *13*, 415.

(13) (a) Perez-Maqueda, L. A.; Criado, J. M. *Solid State Phenom.* **2003**, *90−91*, 509. (b) Lenggoro, I. W.; Panatarani, C.; Okuyama, K. *Mater. Sci. Eng., B* **2004**, *113*, 60.

(14) Urban, J. J.; Yun, W. S.; Gu, Q.; Park, H. *J. Am. Chem. Soc.* **2002**, *124*, 1186.

(15) Niederberger, M.; Garnweitner, G.; Pinna, N.; Antonietti, M. *J. Am. Chem. Soc.* **2004**, *126*, 9120.

10.1021/cm0525961 CCC: $33.50
Published on Web 02/15/2006

thermal and related methods,[16] and precipitation from a precursor solution or gel suspension in a strong alkaline environment.[17] Thermodynamic modeling of the Ti−Sr−H_2O−CO_2 system[18] has been used to assess the conditions corresponding to the formation of $SrTiO_3$ from aqueous solutions. In the absence of CO_2 and at pH > 8, $SrTiO_3$ is the stable phase at 25−100 °C over a wide range of strontium concentrations. Contact with atmospheric CO_2 has to be avoided because of the formation of $SrCO_3$.

As pointed out in previous work about the synthesis of $BaTiO_3$,[19,20] precipitation from a titanium hydroxide gel suspension is very effective for producing particles with controlled sizes. In general, the size distribution of the particles that grow from solution depends on the relative rates of nuclei formation and crystal growth.[21] Nucleation and growth rates are determined by the supersaturation of the solution. In turn, supersaturation is very sensitive to temperature, concentration, and mixing conditions. Crystal aggregation can also contribute substantially to the overall particle-growth process.[21] Growth by the aggregation of small colloidal primary particles produces assemblies called secondary particles. In some cases, the primary nanocrystals attach in a highly oriented fashion to produce single-crystal architectures. This process is termed epitaxial self-assembly as well as oriented aggregation or oriented attachment. The oriented aggregation of primary nanocrystals in bigger particles with a well-defined morphology that sometimes mirrors that of single crystals has been reported for several compounds, including alkaline-earth carbonates,[22] fluoroapatite,[23] $BaSO_4$ and $BaCrO_4$,[24] Co_3O_4,[25] CuO,[26] copper and nickel oxalates,[27] Fe_2O_3,[28] iron and cobalt oxyhydroxides,[29] LaF_3,[30] PbSe and CdTe,[31] SnO_2,[32] TiO_2,[33] ZnO,[34] and tungstates.[35] Several examples of possible architectures generated by the oriented aggregation of building nanoblocks are provided by Cölfen and Antonietti in their recent review.[36] The oriented aggregation of nanoparticles overcomes the classic concept of crystal growth, which is typically thought to occur via atom-by-atom or monomer-by-monomer addition to an existing nucleus.[21] Oriented attachment also provides a convincing explanation for the presence of dislocations and other nanoscale features in small crystals, as discussed by Penn and Banfield.[37] Although the interactions and the mechanisms controlling the self-assembly process are largely unknown, the driving force for aggregation is related to the replacement of solid−liquid interfaces by solid−solid interfaces of lower energy and to the entropy increase resulting from the removal of water and/or adsorbed molecules. In the case of perfectly oriented attachment, the energy gain is at a maximum because no internal surfaces are generated. Even when the attachment is imperfect and defects such as dislocations, twins, stacking faults, and voids are created, the overall energy is significantly lower than that of an aggregate of randomly oriented nanocrystals.

Despite the large practical interest for the production of tailored particles, a systematic investigation on the growth mechanism and morphology of $SrTiO_3$ particles has not yet been carried out. In this work, a detailed study on the synthesis of well-defined $SrTiO_3$ particles by precipitation is presented. The synthesis process can be represented by the overall reaction

$$SrCl_2(aq) + TiOCl_2(aq) + 4NaOH(aq) \rightarrow SrTiO_3(s) + 4NaCl(aq) + 2H_2O(l) \quad (1)$$

where (aq) denotes a salt in aqueous solution. Synthesis was carried out at three different temperatures and several

(16) (a) Leoni, M.; Viviani, M.; Nanni, P.; Buscaglia, V. *J. Mater. Sci. Lett.* **1996**, *15*, 1302. (b) Roeder, R. K.; Slamovich, E. B. *J. Am. Ceram. Soc.* **1999**, *82*, 1665. (c) Um, M.-H.; Kumazawa, H. *J. Mater. Sci.* **2000**, *35*, 1295. (d) Zhang, S.; Han, Y.; Chen, B.; Song, X. *Mater. Lett.* **2001**, *51*, 368. (e) Mao, Y. B.; Banerjee, S.; Wong, S. S. *Chem. Commun.* **2003**, 408.

(17) (a) Diaz-Guemes, M. I.; Gonzalez Carreño, T.; Serna, C. J.; Palacios, J. M. *J. Mater. Sci.* **1989**, *24*, 1011. (b) Ahuja, S.; Kutty, T. R. N. *J. Photochem. Photobiol., A* **1996**, *97*, 99. (c) Kao, C.-F.; Yang, W.-D. *Mater. Sci. Eng, B* **1996**, *38*, 127. (d) Yang, W.-D.; Hsieh, C.-S. *J. Mater. Res.* **1999**, *14*, 3410. (e) Kumar, V. *J. Am. Ceram. Soc.* **1999**, *82*, 2580. (f) Chen, D.; Jiao, X.; Zhang, M. *J. Eur. Ceram. Soc.* **2000**, *20*, 1261. (g) Zhang, S.; Liu, J.; Han, Y.; Chen, B.; Li, X. *Mater. Sci. Eng., B* **2004**, *110*, 11.

(18) Lencka, M. M.; Riman, R. E. *Ferroelectrics* **1994**, *151*, 159.

(19) Testino, A.; Buscaglia, M. T.; Viviani, M.; Buscaglia, V.; Nanni, P. *J. Am. Ceram. Soc.* **2004**, *87*, 79.

(20) Testino A.; Buscaglia, M. T.; Buscaglia, V.; Viviani, M.; Bottino, C.; Nanni, P. *Chem. Mater.* **2004**, *16*, 1536.

(21) Dirksen, J. A.; Ring, T. A. *Chem. Eng. Sci.* **1991**, *46*, 2389.

(22) (a) Cölfen, H.; Qi, L. *Chem.—Eur. J.* **2001**, *7*, 106. (b) Sondi, I.; Matijevic, E. *Chem. Mater.* **2003**, *15*, 1322. (c) Gehrke, N.; Cölfen, H.; Pinna, N.; Antonietti, M.; Nassif, N. *Cryst. Growth Des.* **2005**, *5*, 1317.

(23) Busch, S.; Dolhaine, H.; DuChesne, A.; Heinz, S.; Hochrein, O.; Laeri, F.; Podebrad, O.; Vietze, U.; Weiland, T.; Kniep, R. *Eur. J. Inorg. Chem.* **1999**, 1643.

(24) (a) Yu, S.-H.; Antonietti, M.; Cölfen, H.; Hartmann, J. *Nano Lett.* **2003**, *3*, 379. (b) Cölfen, H.; Mann, S. *Angew. Chem., Int. Ed.* **2003**, *42*, 2350.

(25) He, T.; Chen, D.; Jiao, X. *Chem. Mater.* **2004**, *16*, 737.

(26) (a) Lee, S. H.; Her, Y. S.; Matijevic, E. *J. Colloid Interface Sci.* **1997**, *186*, 193. (b) Liu, B.; Zeng, H. C. *J. Am. Chem. Soc.* **2004**, *126*, 8124. (c) Zhang, Z.; Sun, H.; Shao, X.; Li, D.; Yu, H.; Han, M. *Adv. Mater.* **2005**, *17*, 42.

(27) (a) Jongen, N.; Bowen, P.; Lemaître, J.; Valmalette, J.-C.; Hofmann, H. *J. Colloid Interface Sci.* **2000**, *226*, 189. (b) Pujol, O.; Bowen, P.; Stadelmann, P. A.; Hofmann, H. *J. Phys. Chem. B* **2004**, *108*, 13128.

(28) (a) Park, G.-S.; Shindo, D.; Waseda, Y.; Sugimoto, T. *J. Colloid Interface Sci.* **1996**, *177*, 198. (b) Sugimoto, T.; Itoh, H.; Mochida, T. *J. Colloid Interface Sci.* **1998**, *205*, 42. (c) Niederberger, M.; Krumeich, F.; Hegetschweiler, K.; Nesper, R. *Chem. Mater.* **2002**, *14*, 78.

(29) (a) Banfield, J. F.; Welch, S. A.; Zhang, H.; Thomsen Hebert, T.; Penn, R. L. *Science* **2000**, *289*, 751.(b) Guyodo, Y.; Mostrom, A.; Penn, R. L.; et al. *Geophys. Res. Lett.* **2003**, *30*, 1512. (c) Penn, R. L.; Stone, A. T.; Veblen, D. R. *J. Phys. Chem. B.* **2001**, *105*, 4690.

(30) Cheng, Y.; Wang, Y.; Zheng, Y.; Qin, Y. *J. Phys. Chem. B.* **2005**, *109*, 11548.

(31) (a) Cho, K.-S.; Talapin, D. V.; Gaschler, W.; Murray, C. B. *J. Am. Chem. Soc.* **2005**, *127*, 7140. (b) Tang, Z.; Kotov, N. A.; Giersig, M. *Science* **2002**, *297*, 237.

(32) (a) Yang, H. G.; Zeng, H. C. *Angew. Chem., Int. Ed.* **2004**, *43*, 5930. (b) Lee, E. J. H.; Ribeiro, C.; Longo, E.; Leite, E. R. *J. Phys. Chem. B* **2005**, *109*, 20842.

(33) (a) Penn, R. L.; Banfield, J. F. *Geochim. Cosmochim. Acta* **1999**, *63*, 1549. (b) Polleux, J.; Pinna, N.; Antonietti, M.; Niederberger, M. *Adv. Mater.* **2004**, *16*, 436. (c) Adachi, M.; Murata, Y.; Takao, J.; Jiu, J.; Sakamoto, M.; Wang, F. *J. Am. Chem. Soc.* **2004**, *126*, 14943.

(34) (a) Pacholski, C.; Kornowski, A.; Weller, H. *Angew. Chem., Int. Ed.* **2002**, *41*, 1188. (b) Taubert, A.; Kübel, C.; Martin, D. C. *J. Phys. Chem. B* **2003**, *107*, 2660. (c) Zhang, S. C.; Li, X. G. *Colloid Surf., A* **2003**, *226*, 35.

(35) (a) Liu, B.; Yu, S.-H.; Li, L.; Zhang, F.; Zhang, Q.; Yoshimura, M.; Shen, P. *J. Phys. Chem. B* **2004**, *108*, 2788. (b) Liu, B.; Yu, S.-H.; Li, L.; Zhang, Q.; Zhang, F.; Jiang, K. *Angew. Chem., Int. Ed.* **2004**, *43*, 4745.

(36) Cölfen, H.; Antonietti, M. *Angew. Chem., Int. Ed.* **2005**, *44*, 5576.

(37) (a) Penn, R. L.; Banfield, J. F *Science* **1998**, *281*, 969. (b) Penn, R. L.; Oskam, G.; Strathmann, T. J.; Searson, P. C.; Stone, A. T.; Veblen, D. R. *J. Phys. Chem. B.* **2001**, *105*, 2177.

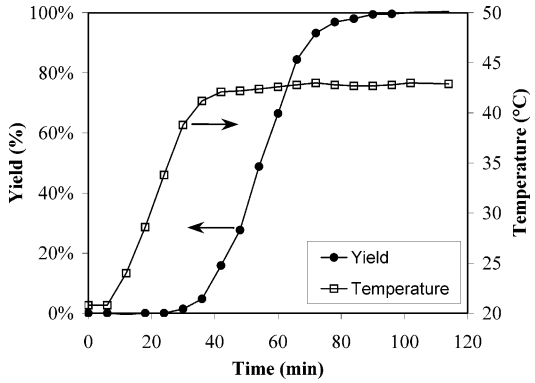

Figure 1. Formation kinetics of $SrTiO_3$ in a batch reactor. The overall titanium concentration is 0.045 mol dm^{-3}. [Sr]:[Ti] = 1.1.

concentrations using batch and tubular reactors. The preliminary kinetic study on the formation of $SrTiO_3$ in a small batch reactor has indicated that the mixing of reactant solutions, the temperature of the suspension, and the heating rate play key roles in determining the particle size distribution. Therefore, the experimental setup has been carefully designed in order to have good control over these parameters.

2. Experimental Section

2.1. Preparation of the Precursor Gel Suspension. An acidic $TiOCl_2$ mother solution (2.8 mol kg^{-1}) was prepared by the drop-by-drop addition of $TiCl_4$ (Acros, 99.9%) to water cooled in an ice bath. The required amount of the $TiOCl_2$ solution was diluted with water and then mixed with a NaOH (Aldrich, 99.9%) solution inside a stirred, closed vessel made of polypropylene. The formation of a highly viscous, gelatinous suspension of Ti hydroxide is immediately observed. An excess of NaOH compared to the stoichiometric amount required by reaction 1 was used. The excess corresponds to $[OH^-] = 1$ mol dm^{-3} after the quantitative precipitation of $SrTiO_3$ and guarantees a nearly constant pH (about 14) during the course of the reaction. The suspension is cooled in an ice bath to ~0 °C, and solid $SrCl_2 \cdot 6H_2O$ (Aldrich, 99.9%) is slowly added while the solution is stirred. Mixing and homogenization of the suspension are carried out by means of a turbine mixer (Ultraturrax). The resulting precursor suspension is kept at 0 °C. This two-step process avoids the premature formation of $SrTiO_3$ nuclei induced by the temperature increase consequent to hydrolysis of $TiOCl_2$. The [Sr]:[Ti] molar ratio in the suspension was 1.1. The titanium concentration in the precursor (i.e., the concentration referred to in the total volume of the gel suspension) is denoted by *c*.

2.2. Preliminary Synthesis of $SrTiO_3$ in a Batch Reactor. Preliminary kinetic experiments on the formation of $SrTiO_3$ were carried out at ~45 °C in a stirred batch reactor (500 mL) made of polypropylene. Some preliminary syntheses were also performed at higher temperatures. The gel suspension was introduced into the reactor, and the vessel was then closed, heated, and kept at constant temperature under stirring. The titanium concentration was $c = 0.045$ mol dm^{-3}. The closed environment limits the formation of $SrCO_3$. The temperature inside the reactor was measured by means of a Pt100 sensor. The formation of $SrTiO_3$ was visually indicated by the gradual transformation from a translucent viscous medium to a white and opaque suspension. The head of the reactor was equipped with 12 plastic (PEEK) tubes and valves. Each tube was connected to a syringe on one side and immersed in the suspension on the other side. At given times (time zero corresponds to the instant the eating was switched on), 20 mL of the suspension was collected, cooled at 0 °C, and sealed in small bottles. The progress of reaction 1 (i.e., yield of $SrTiO_3$) was determined using the methodology described in a previous paper.[20] For this purpose, the collected suspensions were centrifuged, and the strontium concentration in the supernatant was determined by inductively coupled plasma spectroscopy using a specific calibration curve.

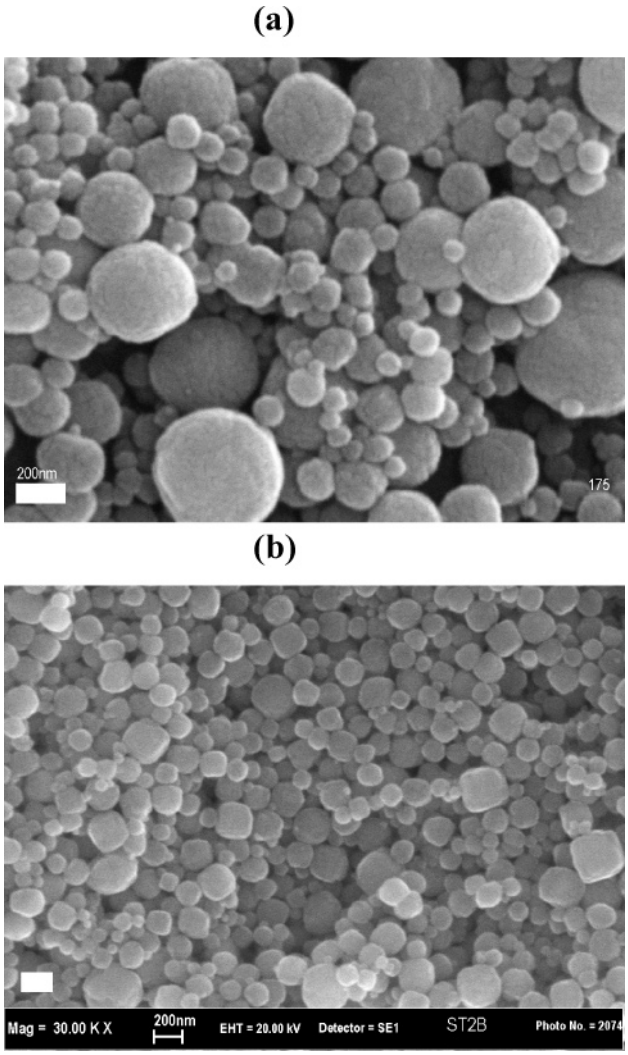

Figure 2. Morphology of $SrTiO_3$ particles precipitated in a batch reactor at 95 °C with a titanium concentration of 0.2 mol dm^{-3} and [Sr]:[Ti] = 1.1 in two different conditions. (a) Powder obtained by mixing a solution of $TiOCl_2$ and $SrCl_2$ with a NaOH solution. (b) Powder obtained from the gel suspension. Bar: 200 nm.

2.3. Synthesis of $SrTiO_3$ in a Tubular Reactor. The tubular reactor consisted of a PTFE tube with an inner diameter of 0.1 cm and length of 20 m immersed in a thermostatic bath. The precursor solution, kept at 0 °C, was injected in the tube by means of a peristaltic pump. The residence time was adjusted between 3 and 22 min by changing the flow rate. In most cases, the residence time was 11 min. The precipitation experiments were conducted at 55, 75, and 95°C using four different titanium concentrations, 0.0225, 0.045, 0.09, and 0.2 mol dm^{-3}. In the latter case, synthesis was performed only at 95 °C. At the end of the tube, the suspension was collected in a bottle cooled in an ice bath.

2.4. Powder Characterization. The final suspension was centrifuged, and the powder was washed and, finally, freeze-dried. The phase-composition was investigated by X-ray powder diffraction (Philips PW1710) usingCo Kα radiation. The crystallite size (d_{XRD}) was estimated from the broadening of the XRD peaks by means of the Scherrer equation, after correction for instrumental

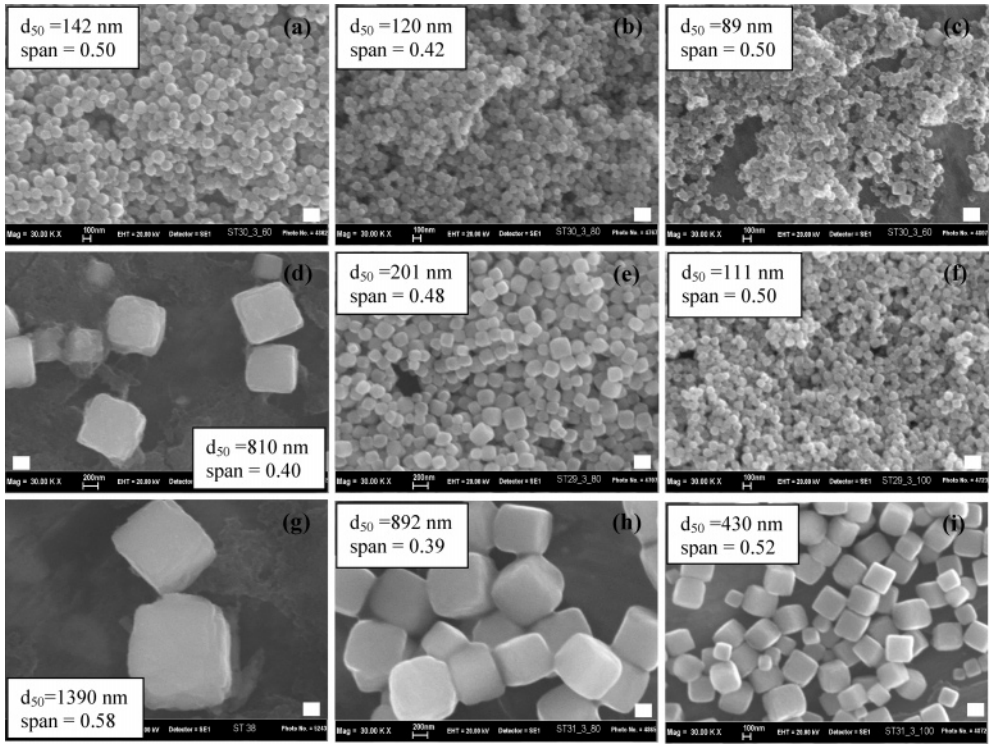

Figure 3. Morphology of $SrTiO_3$ particles precipitated in a tubular reactor. (a) 55 °C, $c = 0.09$; (b) 75 °C, $c = 0.09$; (c) 95 °C, $c = 0.09$; (d) 55 °C, $c = 0.045$; (e) 75 °C, $c = 0.045$. (f) 95 °C, $c = 0.045$; (g) 55 °C, $c = 0.0225$; (h) 75 °C, $c = 0.0225$; (i) 95 °C, $c = 0.0225$. The titanium concentration c is in mol dm^{-3}. Bar = 200 nm.

broadening with a silicon standard, assuming negligible microstrain broadening.

The particle size distribution (PSD) was obtained from the measurement of the diameter of ~1000 particles by scanning electron microscopy (SEM, LEO 1450VP). Three parameters, d_{10}, d_{50}, and d_{90}, were obtained from the PSD. In general, d_p is the diameter corresponding to $p\%$ of the particles in the cumulative particle size distribution. The average particle size was defined as the median diameter (d_{50}) of the PSD. The span of the distribution is given by $(d_{90} - d_{10})/d_{50}$. The internal structure of the particles was studied by high-resolution transmission electron microscopy (HRTEM) and electron diffraction (ED) with a JEOL J2010 microscope operated at 200 kV.

3. Results and Discussion

The formation kinetics of $SrTiO_3$ measured in the batch reactor at 43 °C and $c = 0.045$ mol dm^{-3} is shown in Figure 1 together with the corresponding temperature profile. The sigmoidal shape of the kinetic curve indicates that the reaction is, at least at the early stages, dominated by a nucleation and growth process. The formation of $SrTiO_3$ already starts at around 35 °C, i.e., before the reactor has attained the final temperature (see Figure 1). This observation has a couple of important consequences. First, the reaction kinetics is very sensitive to the heating rate; we have observed that even small variations cause significant changes in the yield vs time curve. This can explain, at least in part, the poor reproducibility of the reaction kinetics determined from the batch reactor. Second, the particle size distribution (PSD) of the final product (100% yield) is rather broad (span ≈ 0.8) because the processes (such as nucleation and aggregation, as will be discussed later) determining the final particle size take place over significant temperature and time intervals. In addition, the formation of $SrTiO_3$ particles is strongly affected by the mixing conditions. For instance, if a solution containing both $SrCl_2$ and $TiOCl_2$ is directly mixed at room temperature with a NaOH solution and then heated at a reaction temperature of 95 °C, the PSD of the final powder is extremely broad relative to that of the product obtained from the gel precursor subjected to the same treatment (Figure 2). The reaction between the chloride solution and NaOH is quite exothermic and determines a temperature increase that causes premature nucleation of $SrTiO_3$ during mixing. Even the shape of the particles is affected by the mixing conditions, with the formation of cubes when starting from the gel precursor and spheres originated by direct mixing. Therefore, to produce well-defined particles of strontium titanate with a narrow particle size distribution, careful control of the experimental conditions is of fundamental importance. This can be accomplished by heating the precursor gel suspension to the reaction temperature in a very short time by means of a tubular reactor. Using a tube with an inner diameter of 0.1 cm, the suspension can be heated to 75 °C within a few seconds.

Precipitation in tubular reactors can be strongly influenced by the inner tube surface. Heterogeneous nucleation of crystals can occur on the tube wall, resulting in incrustation of the inner surface. In turn, these crystals can induce the formation of secondary nuclei and, consequently, variations of the precipitation mechanisms and particle size with time. In the present case, experiments carried out using different combinations of flow rates and tube lengths corresponding to the same residence time did not show significant changes in the particle morphology. In general, the reproducibility of the precipitation experiment with the same tube at different times is good, provided that the tube is properly cleaned and

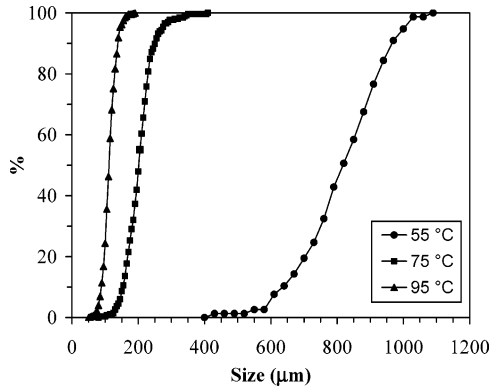

Figure 4. Particle size distribution of $SrTiO_3$ particles synthesized at different temperatures using a titanium concentration of 0.045 mol dm^{-3} and [Sr]:[Ti] = 1.1.

washed after synthesis. Therefore, the inner tube surface seems to have only a minor influence on the precipitation process, at least in the range of experimental conditions investigated in the present study.

Powders synthesized in the tubular reactor have a particle size between 80 (c = 0.2 mol dm^{-3}, 95 °C) and 1400 nm (c = 0.0225 mol dm^{-3}, 55 °C) and a span of 0.4−0.5 (Figure 3). The advantage of using the tubular reactor can be appreciated by comparing Figure 3 with Figure 2. At 55 °C, when c = 0.0225 and 0.045 mol dm^{-3}, complete conversion of the gel precursor in $SrTiO_3$ could not be obtained within the longest residence time (22 min) attainable in the tubular reactor. Therefore, the suspension collected at the end of the tube was further aged in a small batch reactor kept at the same temperature of the tubular reactor until full transformation. The morphology of the particles is in any case cubic, although the particles obtained at high concentrations of 0.09 and 0.2 mol dm^{-3} have a tendency to develop rounded edges. The variation of the average particle size with concentration and temperature is well evident from Figure 3. Some examples of particle size distributions are given in Figure 4. At 55 °C, there is a factor of 10 decrease in particle size (from 1390 to 142 nm) when the concentration is increased. At higher temperatures, a strong effect is observed when the concentration is increased from 0.0225 to 0.045 mol dm^{-3}; with a further increase in the concentration, the variation of particle size is less pronounced. Therefore, at high concentration, the temperature has only a minor effect on the particle size. It is worth noting that, despite the similarities between the two systems, the formation kinetics of $SrTiO_3$ and $BaTiO_3$ as well as the particle morphology are rather different, even when the synthesis is carried out using the same methodology.[19−20,38] The formation of $BaTiO_3$ is observed only at temperatures above 70 °C and quantitative transformation occurs at 80 °C in a reasonable time for concentrations above 0.05 mol dm^{-3}. On the contrary, the quantitative formation of $SrTiO_3$ is observed after 10 min at 40−50 °C for c = 0.045 mol dm^{-3}. The morphology of $BaTiO_3$ corresponds to spheroidal particles with a tendency to form dendritic structures at low concentration.

According to the XRD patterns, the powders consist of cubic $SrTiO_3$ with traces (∼1%) of $SrCO_3$ (see the Supporting Information). The secondary phase mainly originates from the carbonate impurities contained in the raw materials ($SrCl_2 \cdot 6H_2O$ and NaOH). For the finest powder (T = 95 °C, c = 0.2 mol dm^{-3}), the particle size measured by SEM corresponds well to the XRD size (see the Supporting Information). HRTEM observation shows single-crystal nanoparticles with very smooth surfaces. Powders obtained at low concentrations display a completely different microstructure. Despite the fact that the apparent morphology (Figure 3) is that of single crystals, it is apparent from Figure 5 that the particles consist of aggregates of small rounded nanocrystals 4−5 nm in diameter. As revealed by the parallelism of the lattice fringes, all the nanocrystals are aligned along the same crystallographic direction and, therefore, the ED pattern of the particle corresponds to that of a single crystal. A lower contrast between the crystallites indicates that nanopores and/or an amorphous phase separate many primary particles (Figure 5b). Slight misorientations between the primary nanoparticles and dislocations are also observed. These nanometer-length scale features, as well as the dimples and creases observed at the surface, strongly

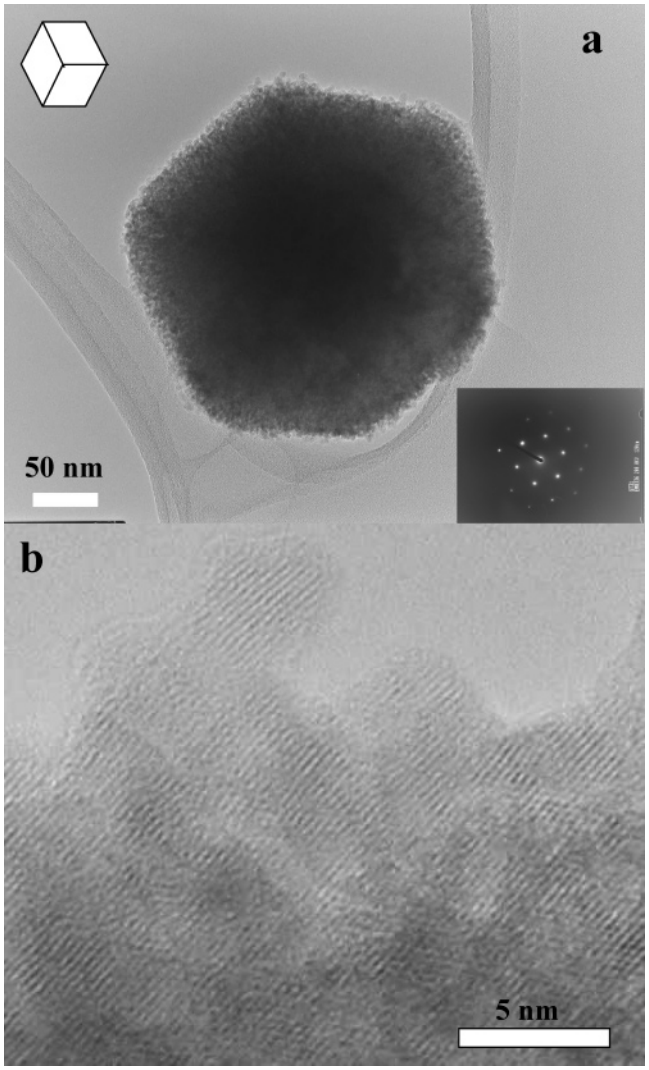

Figure 5. Morphology (HRTEM) of a $SrTiO_3$ particle (95 °C, c = 0.0225 mol dm^{-3}). (a) The particle as seen from a vertex of the cube, as depicted in the sketch. The inset shows the ED pattern of the whole particle. (b) Magnification of one of the edges. Dislocations and slight misalignments across some interfaces are apparent when the micrograph is viewed along a low angle.

(38) Testino, A.; Buscaglia, V.; Buscaglia, M. T.; Viviani, M.; Nanni, P. *Chem. Mater.* **2005**, *17*, 5346.

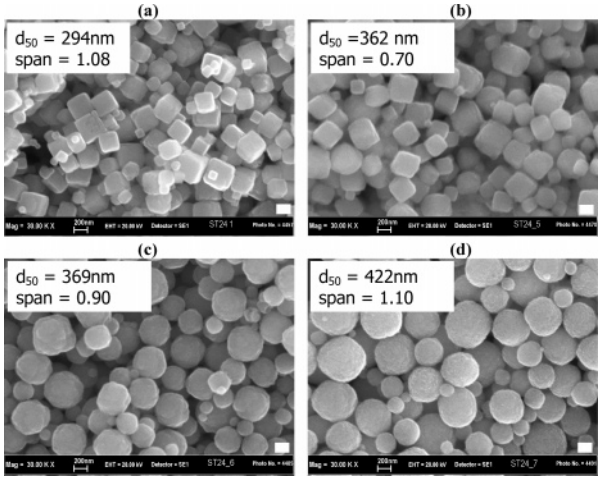

Figure 6. Influence of sodium citrate (SC) on the morphology of $SrTiO_3$ particles precipitated in a batch reactor at 80 °C with a titanium concentration (c) of 0.0125 mol dm^{-3}. [Sr]:c = 1.1. (a) [SC]:c = 0; (b) [SC]:c = 0.011; (c) [SC]:c = 0.084; (d) [SC]:c = 0.79. Bar: 200 nm.

suggest that the particles of Figure 3 originated from the epitaxial self-assembly (also called oriented attachment or oriented aggregation) of small primary nanocrystals. Dislocations and small misalignments across some interfaces are the consequence of imperfect oriented attachment of the primary building units.[37] According to the substructure revealed by TEM, the XRD patterns of the powders show broadened peaks (see the Supporting Information). The size of the coherently diffracting domains, calculated from the Scherrer equation, is on the order of some tens of nm.

The influence of sodium citrate (SC, Aldrich, 99.9%) on the morphology of $SrTiO_3$ particles has been investigated in the batch reactor at 80 °C, c = 00125 mol dm^{-3}, for different [SC]:c molar ratios. The aging time was 24 h. Sodium citrate was added to the $TiOCl_2$ solution before hydrolysis with NaOH. For [SC]:$c \leq 0.01$, the particle morphology is still cubic with a moderate increase in the average particle size (from 290 to 360 nm) and a significantly narrower PSD (span = 0.7). When [SC]:c = 0.08 and 0.8, the particles become spherical and the size is increased up to 420 nm, as shown in Figure 6. The increase in SC concentration gives rise to a broader PSD. The influence of the cation concentration on the morphology of the $SrTiO_3$ particles obtained in the presence of sodium citrate was studied for [SC]:c = 1 and c = 0.0125, 0.1, and 0.33 mol dm^{-3}. With increasing concentration, the particle size decreases from 440 to 180 nm, whereas the morphology remains spherical, as shown in Figure 7. Observation by HRTEM shows (Figure 8), like the particles obtained without the addition of SC, that the particles consist of epitaxial aggregates of small nanocrystals 4−5 nm in diameter. The single-crystal ED pattern and the alignment of the lattice fringes indicate that the nanocrystals share a single and common crystallographic orientation. Lower contrast between crystallites indicates the presence of pores, amorphous material and/or adsorbed sodium citrate layers. Several dislocations and inner interfaces originating from small misalignments of the lattice fringes are apparent in Figure 8. According to XRD patterns, the powders consist of cubic $SrTiO_3$ with traces of $SrCO_3$. The XRD peaks appear significantly broadened (see the Supporting Information), in agreement with the nanocrystalline substructure of the

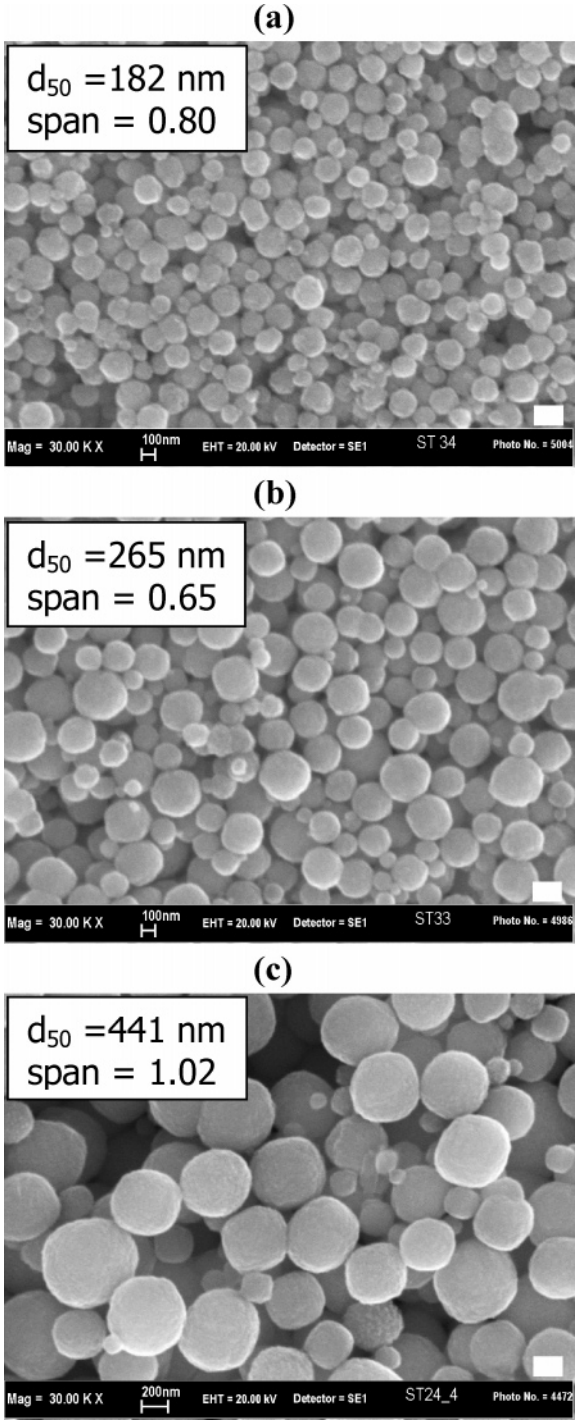

Figure 7. Influence of titanium concentration (c) on the morphology of $SrTiO_3$ particles precipitated at 80 °C in a batch reactor in the presence of sodium citrate (SC). [SC]:c = 1; [Sr]:c = 1.1. (a) c = 0.33 mol dm^{-3}; (b) c = 0.1 mol dm^{-3}; (c) c = 0.0125 mol dm^{-3}. Bar: 200 nm.

particles. The dimension of the coherently diffracting domains is ∼20 nm, if exclusive size broadening is assumed (Scherrer formula). Overall, the particles obtained in the presence of SC appear to be more disordered and defective than the cubic mesocrystals produced in the absence of additives.

The process of $SrTiO_3$ particle construction is likely to occur in two main stages. At first, nucleation and limited growth occur from the supersaturated gel suspension to give 4−5 nm nanocrystals. These primary nanocrystals then aggregate in a highly oriented fashion to produce secondary

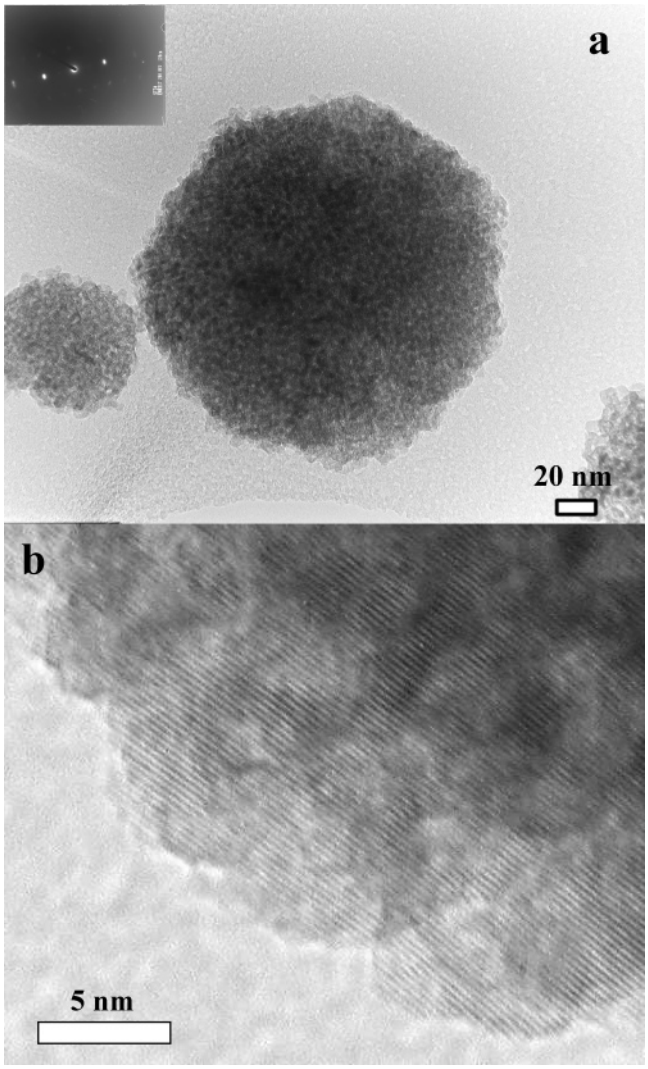

Figure 8. Morphology (HRTEM) of a $SrTiO_3$ particle (80 °C, $c = 0.33$ mol dm^{-3}) synthesized in the presence of sodium citrate ([SC]:$c = 1$). The inset of part (a) shows the ED pattern of the whole particle. A magnification of the surface region is shown in part (b). Dislocations and slight misalignments across some interfaces are apparent when the micrograph is viewed along a low angle.

particles on the submicrometer length scale. As the formation kinetics of $SrTiO_3$ is rather slow (Figure 1), the two processes probably occur simultaneously and the secondary particles grow by the progressive addition of freshly formed building blocks. Different from previous investigations on different systems,[24,36] the growth of the $SrTiO_3$ cubic particles by the oriented aggregation of small nanocrystals as observed in the present study is a spontaneous process not induced or mediated by adsorbed organic molecules or polymers. Because the diameter (4−5 nm) of the primary nanocrystals seems to be rather independent of the experimental conditions (concentration, temperature, addition of sodium citrate), it can be concluded that the size of the final particles is mainly determined by the assembly process. Higher temperatures and higher concentrations lead to particles composed of a smaller number of primary units. Considering the explored size interval (Figure 3), the number of primary units per particles ranges between 10^4 and 10^6. As an example, the particles shown in Figures 5 and 8 consist of about 10^5 nanocrystals. These are remarkable numbers, because in many of the cases reported in the literature, secondary particles generated by oriented attachment comprise few units to few hundreds of building blocks.

The above results represent a clear example of the possibility for controlling the self-assembly process by changing the concentration and temperature of the solution. The natural tendency of the $SrTiO_3$ nanocrystals to self-organize in the investigated experimental conditions could be further exploited by using templates and/or suitable organic molecules or polymers that adsorb at the solid−liquid interface. We have recently shown that $SrTiO_3$ nanocrystals spontaneously assemble at the surface of $BaTiO_3$ spherical templates with the formation of core−shell structures.[39] Therefore, the design and realization of a range of 1D, 2D, and 3D solid shapes and architectures is not an unrealistic goal.

4. Summary and Conclusions

Well-defined $SrTiO_3$ particles with a narrow size distribution were synthesized by precipitation from an aqueous gel suspension prepared by hydrolyzing a $TiOCl_2$ solution with NaOH and adding $SrCl_2$. The experimental results reported in this study provide strong evidence that orientated aggregation (also called oriented attachment) of small (4−5 nm) nanocrystals is the dominant growth mechanism for the formation of defective single-crystal cubic $SrTiO_3$ particles (mesocrystals) in a wide range of temperatures (45−95 °C) and concentrations (0.02−0.1 mol dm^{-3}). The size of the particles can be tailored in the range 80−1400 nm by varying the synthesis conditions. The observed broadened XRD peaks clearly indicate that the size of the coherently diffracting domains is much smaller that the apparent size of the particles. The primary nanocrystals can be revealed, at least in part, in HRTEM images of the final particles by the presence of defects and peculiar nanometer-length scale features, such as small misorientations or the lattice fringes, dislocations, pores, and/or amorphous material, dimples, and creases at the surface of the secondary particles. The addition of citric acid produces spherical particles that still result from the oriented aggregation of primary nanocrystals.

Oriented aggregation represents a fascinating and powerful tool to design and realize materials with the desired shape, anisotropy and properties. It is expected that the self-assembly process could be directed to the production of a range of shapes and architectures by the use of organic molecules or polymers that selectively adsorb on specific solid surfaces and/or by employing suitable templates. Because $SrTiO_3$ becomes ferroelectric with small additions of Ba or Ca, the self-assembly process would lead to a new strategy for the realization of more- or less-complex 1D, 2D, and 3D ferroelectric structures with new or different properties.

Supporting Information Available: X-ray diffraction patterns (Co Kα radiation) corresponding to $SrTiO_3$ powders prepared in different conditions (Figures S1−S4) (pdf). This material is available free of charge via the Internet at http://pubs.acs.org.

CM0525961

(39) Buscaglia, M. T.; Viviani, M.; Zhao, Z.; Buscaglia, V.; Nanni, P. *Chem. Mater.* Submitted (October 2005).